Determination of the magnetic structures of the field-induced phases of $HoMnO_3$

P. J. Brown and T. Chatterji
Institut Laue-Langevin, Boîte Postale 156, 38042 Grenoble Cedex, France
(Received 14 September 2007; revised manuscript received 1 December 2007; published 7 March 2008)

We have determined the magnetic structure of the field-induced phases of the multiferroic hexagonal manganite $HoMnO_3$ by combining integrated intensity data, collected with unpolarized neutrons on a single crystal, with measurements of the polarization dependence of the intensities of the diffraction peaks from the same crystal. The present investigation shows that the magnetic structure of $HoMnO_3$ changes, apparently nearly continuously, with increasing field from the zero field antiferromagnetic (AF1) phase ($P6'_3cm'$) to a ferromagnetic (F2) phase ($P6_3c'm'$) in which the triangular configuration of Mn moments in the (001) plane is maintained. There is also a significant variation with field in the ordered moments of Ho2 and Mn in the AF1 and F2 phases, respectively. We show that the structures of the field-induced phases cannot be determined completely from the integrated intensity measurements alone.

DOI: 10.1103/PhysRevB.77.104407 PACS number(s): 75.30.Ds, 75.25.+z, 75.80.+q

I. INTRODUCTION

The magnetoelectric effect, namely, induction of electric polarization by a magnetic field or vice versa, has been known for a long time.[1–3] Although, in principle, the effect could be very useful in device applications, its magnitude in classical magnetoelectric materials is too small and the initial interest in the effect decayed quite rapidly. Recently, however, renewed interest has been generated following the discovery of relatively large magnetoelectric effects in three classes of rare-earth manganites: These comprise both the hexagonal[4] and the orthorhombic[5,6] $RMnO_3$ (R=rare-earth element) series and the orthorhombic RMn_2O_5 compounds.[7] Among hexagonal manganites, the largest effect[4] is found in $HoMnO_3$, which is ferroelectric below T_C=875 K (Ref. 8) and in which the Mn^{3+} order antiferromagnetically below T_N=75 K (Ref. 9) and the Ho^{3+} below T_{Ho}=4.6 K.[10] $HoMnO_3$ has been reported to undergo several transitions at low temperature induced by electric and magnetic fields.[11–13] Lottermoser *et al.*[4] demonstrated that its magnetic structure can be controlled by an external electric field: Ferromagnetic ordering is reversibly switched on and off via magnetoelectric interactions. The process was monitored using magneto-optical techniques, and its microscopic origin was revealed by neutron and x-ray diffraction. The rather complex (H,T) phase diagram derived for $HoMnO_3$ from dielectric anomalies[13] is shown in Fig. 1. In a neutron diffraction study,[11] some of these phase changes were also evident in the field dependence of $hk0$ reflection intensities, but the data were insufficient to derive the changes in structure. The present experiment was undertaken to try to determine the magnetic structures in the distinct regions of the (H,T) phase diagram. To this end, we have made measurements of both integrated reflection intensities and their dependence on neutron polarization (polarized neutron asymmetries) using a single crystal of $HoMnO_3$ under magnetic fields between 0 and 5 T applied parallel to [001] at temperatures in the range of 2–7 K. We note that a unique determination of a magnetic structure is not always possible from unpolarized neutron intensity measurements alone, and this is particularly true for the homometric magnetic structures of hexagonal manganites. In such cases, information provided by polarized neutron measurements can be very helpful.[14] This study of the magnetic structure of the field-induced phases of $HoMnO_3$ provides a good example of this situation. As will be seen, the symmetry observed in the polarized neutron data precludes any structures that do not have the full symmetry of the paramagnetic phase. Structures conforming to this symmetry have been refined from the unpolarized neutron data, and their relationship to the applied field deduced from the signs of the polarized asymmetries.

II. EXPERIMENT

The integrated intensity measurements were made using the single-crystal diffractometer D15 of the Institut Laue-Langevin in the normal beam mode with the crystal mounted in a 6 T superconducting magnet with [001] parallel to both

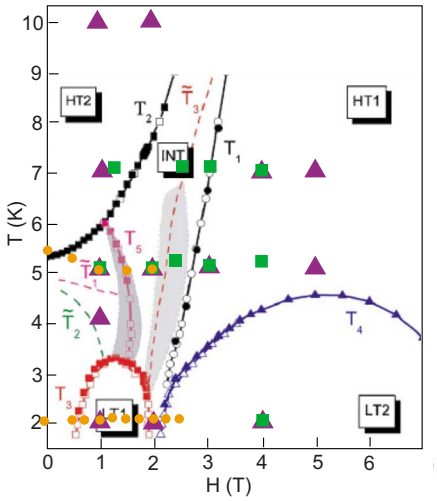

FIG. 1. (Color online) (H,T) phase diagram for $HoMnO_3$ derived from dielectric anomalies (Ref. 13). The H,T points at which restricted sets of integrated intensities were measured are shown by orange (gray) circles, those for the extended sets by green (gray) squares. The purple (gray) triangles mark points at which the polarized neutron asymmetries were measured.

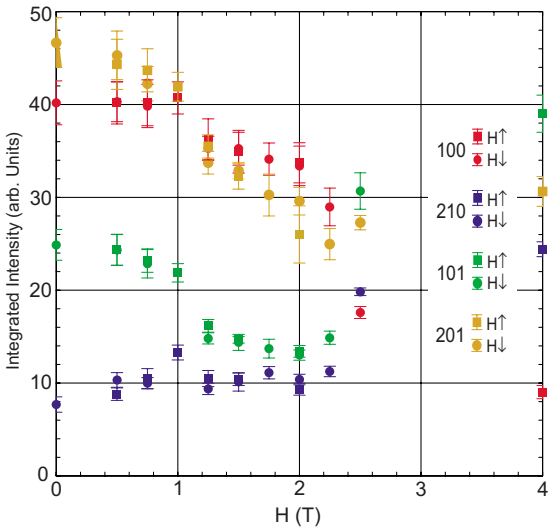

FIG. 2. (Color online) Magnetic field dependence of the integrated intensities of the 100, 210, 101, and 201 reflections from $HoMnO_3$ at 2 K.

the field and ω axes. The angular aperture of the magnet allowed access to reflections with $l=0$, 1, and 2. Restricted data sets containing 14 independent reflections $l=0,1$ were measured at the points marked by filled circles in Fig. 1. More extended sets containing 33 independent reflections $l=0,1,2$ were obtained at the points marked by squares. The magnetic field dependence of the intensities of the 100, 210, 101, and 201 reflections at 2 K is shown in Fig. 2. These reflections are almost entirely magnetic in origin; for 100 and 210 the nuclear scattering is small, and for 101 and 201 it is forbidden by symmetry. Measurements were made with increasing and decreasing field, as indicated, but the time needed to collect each data set varied from 4 to 12 h. On this time scale, any hysteretic effects are close to the limits of accuracy of the measurements.

Additional information about the way in which the magnetic structure responds to an applied field can be obtained by measuring the polarization dependence of the reflection intensities. For magnetic structures with zero propagation vector, magnetic and nuclear scattering contribute to the same reflections, and the Bragg intensity for neutrons with polarization $\mathbf{P}$ is given by[14]

$$I^{\mathbf{P}}(\mathbf{k}) \propto |N(\mathbf{k})|^2 + |\mathbf{M}_\perp(\mathbf{k})|^2 + 2\Re \mathbf{P}\cdot\mathbf{M}_\perp(\mathbf{k})N^*(\mathbf{k}), \quad (1)$$

where $N(k)$ is the nuclear structure factor for the reflection with scattering vector $\mathbf{k}$ and $\mathbf{M}_\perp(\mathbf{k})$ is its magnetic interaction vector; $\Re$ signifies the real part. If $\mathbf{P}$ is parallel to the direction of applied field (z) and $M_z(\mathbf{k})$ is the z component of $\mathbf{M}_\perp(\mathbf{k})$, then the asymmetry A in the intensities I^+ and I^- scattered with polarization parallel (+) and antiparallel (−) to z is

$$A = \frac{I^+ - I^-}{I^+ + I^-} = \frac{2\Re P M_z(\mathbf{k})N^*(\mathbf{k})}{|N(\mathbf{k})|^2 + |\mathbf{M}_\perp(\mathbf{k})|^2}, \quad (2)$$

where P is a scalar parameter, which measures the effective polarization: a product of the initial beam polarization, depolarization by the sample, and any necessary average over differently oriented domains. The intensity asymmetry therefore yields information about the relative phases of the nuclear and magnetic scattering, which is not contained in the unpolarized neutron intensities that depend simply on $|N(\mathbf{k})|^2+|\mathbf{M}_\perp(\mathbf{k})|^2$.

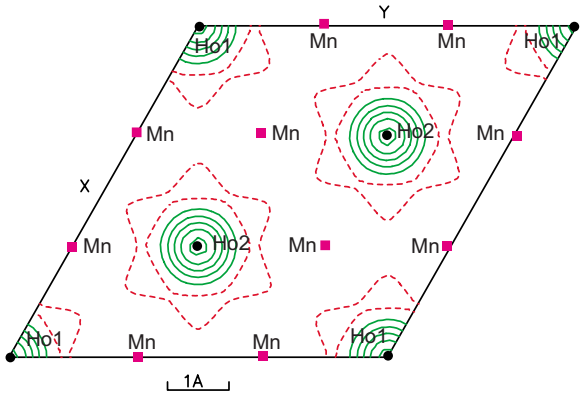

FIG. 3. (Color online) Projection on the (001) plane of the magnetization aligned parallel to [001] in $HoMnO_3$ by a field of 1 T at 2 K.

The polarization dependence of the reflection intensities was measured using the polarized neutron diffractometer D3 of the Institut Laue-Langevin, again using normal beam geometry with the crystal magnetized in the [001] direction. The polarization dependence of the peak intensities of all accessible reflections with $\sin\theta/\lambda < 0.45$ Å^{-1}, and $l=0,1,2$ was measured at each of the points in the (H,T) phase diagram marked by the purple triangles in Fig. 1. The lowest field value of 1 T is the minimum field required to retain the neutron polarization when using the superconducting magnet on D3. The polarized neutron asymmetry A was calculated for each reflection. Values of A significantly different from zero were observed even at the lowest field, being particularly significant in the 111 and 112 types. The hexagonal equivalence of the asymmetries, within the experimental precision, was preserved at all temperatures and fields.

III. ANALYSIS OF THE DATA

Analysis of the $hk0$ asymmetries is straightforward because the [001] projection of space group $P6_3cm$ is centrosymmetric. $\mathbf{k}$ is perpendicular to M_z for all $hk0$ reflections so $M_z(\mathbf{k})=\mathbf{M}_\perp(\mathbf{k})$ and can be obtained from the relationship

$$A = 2M_z(\mathbf{k})N(\mathbf{k})/[|\mathbf{M}_\perp(\mathbf{k})|^2 + N(\mathbf{k})^2]$$

using values of the nuclear structure factors calculated from the known crystal structure. A Fourier summation using these components as coefficients yields a projection on the (001) plane of the the magnetization parallel to [001]. The map obtained using the data collected at 2 K in 1 T is shown in Fig. 3; it suggests that there is no significant z component of magnetization at the Mn sites and that the Ho1 and Ho2 atoms are magnetized almost equally parallel to [001].

Using this result as a guide, a model in which the z components of magnetization are due to a partial ferromagnetic

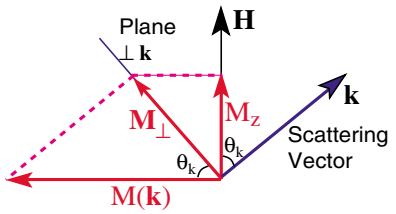

FIG. 4. (Color online) A magnetic structure factor $\mathbf{M_k}$ in the xy plane has a magnetic interaction vector $\mathbf{M}_\perp$ perpendicular to $\mathbf{k}$. If $\mathbf{k}$ is not perpendicular to either z or $\mathbf{M_k}$, $\mathbf{M}_\perp$ will have a finite z component M_z.

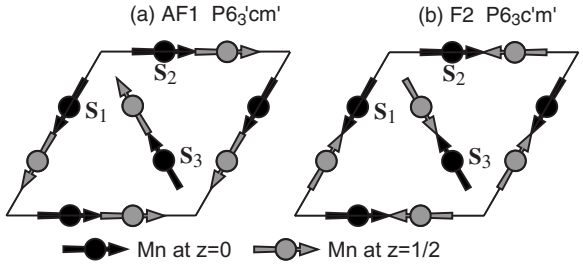

FIG. 5. Schematic representation of the Mn moment directions in the AF1 and F2 phases of $HoMnO_3$.

alignment of local moments at the Mn, Ho1, and Ho2 sites was fitted by least squares to the asymmetries A of the $hk0$ reflections in each of the data sets measured. The results showed that there is no significant magnetization parallel to [001] associated with the Mn atoms at any of these (H,T) points. Significant magnetization is aligned at the Ho1 and Ho2 sites; between 2 and 10 K, this magnetization is almost independent of temperature. The values for the Ho1 and Ho2 sites do not differ by more than 10%, and they are given to within the experimental accuracy by $\mu_{\mathrm{Ho}}=0.25H$ with μ in μ_B and H in T.

The model fitted to the $hk0$ asymmetry data corresponds to a structure with magnetic space group $P6_3c'm'$. It is the only one retaining the full symmetry of the crystal structure, which allows ferromagnetic alignment of the moments on both Ho sites. It is, however, inadequate to account for the asymmetry measurements with $l\neq 0$. For these reflections, not only are the structure factors complex, but, as indicated in Fig. 4, there may also be z components of $\mathbf{M}_\perp$ due to Mn even though the Mn moments lie in the plane perpendicular to z. Expressions for the magnetic structure factors are developed in Appendix A. For 111, the nuclear structure factor is almost purely imaginary, and the magnetic structure factor due to the triangular array of Mn atoms is zero. The Ho magnetic structure factor is also almost purely imaginary and proportional to the difference between the Ho moments in the layers separated by $c/2$. The nonzero value measured for A_{111} therefore implies some inequality or antiparallel alignment of such pairs of moments. On the other hand, the asymmetry measured for the 202 reflection, to which the aligned Ho moments contribute very little, increases strongly with increasing field. Its nuclear structure factor is again almost purely imaginary, so the increase must be due to an increasing imaginary contribution from Mn. For M_z to be finite, its magnetic structure factor must have an imaginary component parallel to 200. This requires antiparallel alignment of the Mn layers with the moments oriented parallel to the axis on which they lie, $\mathbf{S}_3-\mathbf{S}_1\|(100)$. This is the configuration corresponding to $P6_3c'm'$ [Fig. 5(b)]. These observations are consistent either with a multiphase state containing both ferromagnetic $(P6_3c'm')$ and antiferromagnetic $(P6_3'cm')$ regions or with a structure in which the 6_3 symmetry is broken so that the Ho layers separated by $c/2$ are no longer equivalent. This latter possibility is ruled out by the consistent hexagonal equivalence of the asymmetry measurements. As shown in Appendix B, any nonhexagonal model leads to polarized neutron asymmetries that differ for reflections related by the missing symmetry element, and the contribution of the nonhexagonality to the asymmetry averages to zero when the twin domains related by this symmetry are equally populated.

A two phase model consisting of a mixture of ferromagnetic (F2) and antiferromagnetic (AF1) regions has been fitted to the integrated intensity and asymmetry data. The AF1 phase is the zero field structure stable below 50 K with magnetic space group $P6_3'cm'$.[15] The ferromagnetic F2 regions have the magnetic space group $P6_3c'm'$ with ferromagnetically aligned Ho moments; the Mn moments maintain their triangular configuration, but the coupling between Mn layers at $z=0$ and $=\frac{1}{2}$ is reversed with respect to the zero field structure, as in Fig. 5. In the most general fit to this model, the parameters that can be refined are the moments associated with Mn, Ho1, and Ho2 atoms in each phase and the fraction of the F2 phase. For the asymmetry data, there are also two polarization parameters, one for each phase, which measure the product of the beam polarization with the fractional difference in the populations of 180° domains. The $hk0$ asymmetry data show that the Ho1 and Ho2 moments in the F2 phase are nearly the same; in the fitting procedure, they were constrained to be equal, which improved the stability of the refinements. A good fit with the integrated intensity data, giving crystallographic R factors $\approx 6\%$ and $\chi^2=2-11$, was obtained with this model for all the H,T points at which measurements had been made. The results are displayed in Table I.

For the points at which both both polarized and unpolarized data were measured, a qualitative agreement could be obtained with the asymmetry data using the parameters obtained from the integrated intensity fit and refining just the two polarization parameters. The values obtained for the Mn and Ho1 moments in the AF1 phase and for the Ho moments in the F2 phase vary rather little with field. Figure 6 shows values obtained for the Ho2 moment in the AF1 phase and the Mn moment in the F2 phase, plotted as a function of field and compared with the fraction of the F2 phase present. The fraction of F2 increases apparently continuously with increasing field and saturates at $\approx 95\%$ in fields above 3 T. The Mn F2 moment at 2 K appears to peak between 0.5 and 1 T and pass through a minimum around 2 T before saturating at $\approx 3\mu_B$ above 2.5 T. It is this behavior which is responsible for the variation in the 210 intensity reported previously.[11] The Ho2 moment in the AF1 phase falls with increasing field to nearly zero at 2.5 T. The values obtained at higher fields are unreliable because the fraction of the AF1 phase present

TABLE I. Results obtained from refinements of the two phase model from integrated intensity data measured as a function of temperature and field.

H (T)	T (K)	AF1			F2			R_{cryst}	χ^2	N_{obs}
		Mn (μ_B)	Ho1 (μ_B)	Ho2 (μ_B)	Mn (μ_B)	Ho (μ_B)	%			
0.00	2.06	3.38(8)	4.16(7)	1.54(9)	−1.4(1)	3.86(1)	5(4)	5.00	1.70	14
0.50	2.01	3.7(1)	4.1(1)	1.7(2)	−2.1(2)	3.86(1)	15(5)	5.70	3.50	14
0.50	2.07	3.6(1)	4.2(2)	1.6(2)	−1.7(2)	3.86(1)	11(6)	5.20	4.60	14
0.75	2.07	3.84(9)	4.03(9)	1.5(1)	−1.9(1)	3.86(1)	17(3)	4.50	1.30	14
0.75	2.06	3.7(2)	4.0(2)	1.5(2)	−1.8(2)	3.86(2)	14(6)	5.80	4.60	14
1.00	2.06	4.3(2)	4.0(2)	1.3(2)	−2.5(2)	3.86(2)	26(6)	5.20	5.80	14
1.25	2.06	4.1(2)	3.6(2)	1.0(1)	−1.2(2)	3.85(3)	44(5)	5.30	7.90	14
1.25	2.06	4.1(1)	3.6(1)	1.0(1)	−1.3(1)	3.86(1)	38(4)	4.80	2.60	14
1.50	2.06	4.3(1)	3.5(1)	0.94(9)	−1.2(1)	3.85(2)	45(4)	3.90	3.60	14
1.50	2.06	4.2(1)	3.5(1)	1.1(1)	−1.2(1)	3.86(1)	42(3)	4.80	2.70	14
1.75	2.06	4.4(2)	3.4(1)	0.8(1)	−1.4(1)	3.86(1)	51(5)	5.60	3.90	14
2.00	2.07	4.2(1)	3.44(9)	0.8(1)	−1.1(1)	3.86(1)	53(4)	4.80	2.10	14
2.00	2.07	4.3(2)	3.3(1)	0.7(2)	−1.2(1)	3.86(1)	53(5)	5.90	4.30	14
2.25	2.07	4.4(1)	3.5(1)	0.4(1)	−1.33(9)	3.86(1)	69(2)	4.50	2.20	14
2.50	2.06	2.9(1)	3.2(1)	0.1(2)	−2.64(6)	3.93(3)	78(13)	4.90	4.00	14
4.00	2.07	4.51(6)	4.18(7)	−1.3(1)	−3.0(1)	3.9(2)	96(7)	5.80	2.70	33
0.00	5.50	3.3(2)	2.93(9)	0.87(6)	−1.45(6)	3.84(1)	8(7)	5.70	4.90	14
0.50	5.30	4.04(6)	3.27(6)	1.01(6)	−0.2(1)	3.85(1)	27(3)	4.30	1.80	14
1.00	5.00	4.4(1)	3.2(1)	1.0(1)	−1.3(1)	3.86(1)	36(4)	5.10	3.10	14
1.50	5.00	4.7(2)	3.3(2)	0.6(3)	−1.1(2)	3.86(2)	51(6)	5.70	10.20	14
2.00	5.11	3.6(1)	3.3(1)	0.7(1)	−1.1(1)	3.0(2)	47(3)	4.90	2.40	33
2.00	5.01	5.4(2)	5.2(2)	1.4(2)	−0.6(3)	2.4(3)	75(4)	10.90	7.90	33
2.00	5.00	4.3(1)	3.0(1)	0.73(9)	−0.87(8)	3.86(1)	56(3)	5.70	3.50	14
2.40	5.11	3.6(1)	3.0(1)	0.4(1)	−1.53(7)	3.3(2)	63(3)	5.20	2.10	33
3.00	5.11	3.75(7)	4.89(8)	0.24(5)	−2.9(1)	3.8(2)	96(10)	7.20	2.80	33
4.00	5.11	3.2(1)	5.4(2)	−0.2(2)	−3.0(1)	3.9(2)	95(8)	7.00	4.30	33
1.20	7.10	3.6(2)	3.3(2)	0.8(1)	−1.2(2)	2.4(2)	22(4)	5.50	3.40	33
2.50	7.11	3.7(1)	3.3(1)	0.6(1)	−1.39(9)	3.1(1)	65(2)	5.30	1.60	33
3.00	7.10	4.0(1)	4.2(2)	1.1(3)	−2.9(1)	3.5(3)	96(13)	7.80	5.70	33
4.00	7.10	4.56(4)	4.08(5)	−1.24(9)	−2.98(7)	3.9(1)	96(6)	6.50	1.50	33

is very small. The Ho moments in the F2 phase have a nearly constant value of $\approx 3.86\mu_B$ and only begin to diminish at 7 K in lower fields. The increase with field of the aligned Ho magnetization deduced from the $hk0$ asymmetries is due to the increasing fraction of the F2 phase present. This value never reaches the full $3.86\mu_B$ because of the depolarization effect implied by $P_f \ll 1$.

Table II shows the observed and calculated asymmetries at 2 K. The differences, which are in many cases much larger than the errors estimated from counting statistics, are probably due both to inadequacies in the extinction model and to multiple scattering. The largest asymmetries are measured for reflections whose nuclear scattering is rather weak, and these are the ones most sensitive to multiple scattering. For the stronger nuclear reflections, extinction is important; the model obtained in our previous study[15] gives factors of up to 50% in the strong reflections. The observed asymmetry depends on the relative cross sections for opposite polarization states in mosaic blocks within which the magnetic structure is coherent. These may not have the same size as the blocks in which the nuclear structure is coherent, and this size will probably vary as the AF1 phase transforms to F2 with increasing field. On the other hand, the qualitative agreement between observation and calculation and, in particular, the accordance of their signs, gives confidence in the model. It should be emphasized that the structure with magnetic group $P6_3cm$ proposed previously[4] for the low field, low temperature phase predicts zero asymmetry in the 111 reflections and a large value for 211.

IV. DISCUSSION

The finite value of $A(111)$ shows that the populations of the two 180° domains in the AF1 phase are unequal, and its sign determines which of the two is favored in a magnetic field parallel to [001]. This choice is probably determined by

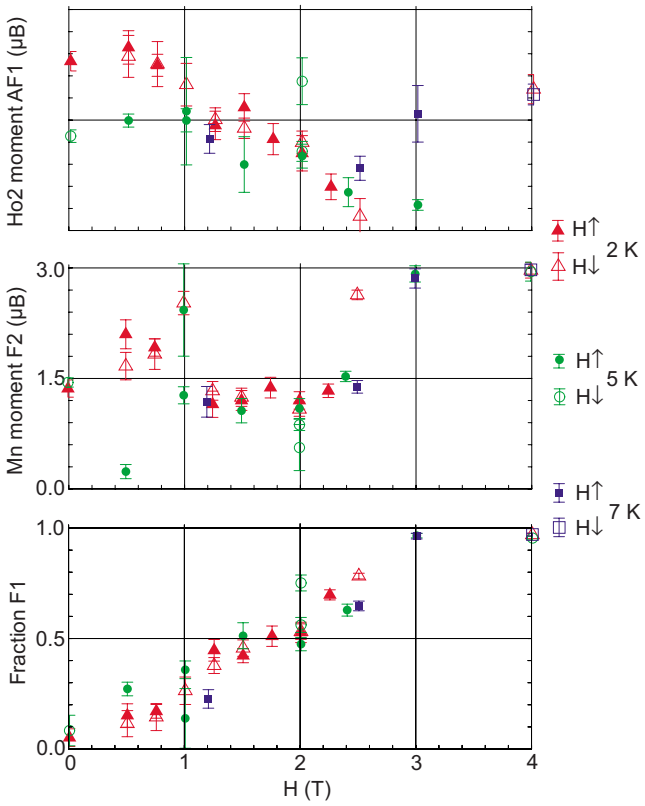

FIG. 6. (Color online) Variation with field of the ordered moments of Ho1 in the AF1 phase and Mn in the F2 phase compared with the fraction of the F2 phase present.

the polar character of the Ho coordination polyhedra; that of Ho1 is illustrated in Fig. 7.

For Ho1, the polarity of the coordination can be characterized by the direction of the unique Ho1–O3 bond, which is parallel to [001] for all Ho1 atoms of one racemic twin and to $[00\bar{1}]$ for the other. The sign of $A(111)$ suggests that the Ho1 moments are slightly larger when they are parallel to this direction than when they are antiparallel. The coupling between the Mn and Ho moments then ensures that, in an

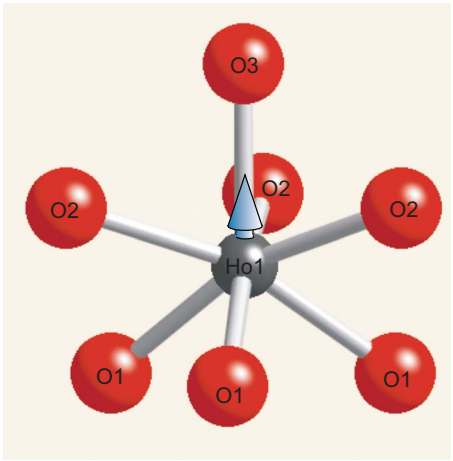

FIG. 7. (Color online) The polar coordination polyhedron of oxygen around the Ho1 atoms in $HoMnO_3$.

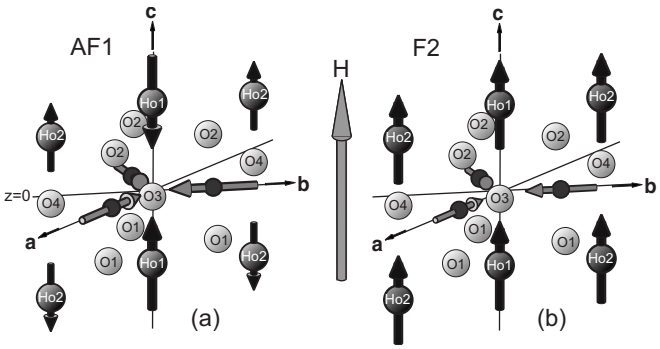

FIG. 8. Schematic drawing of a fragment of the magnetic structures of the AF1 (a) and F2 (b) phases of $HoMnO_3$ around $z=0$ showing the relative orientations of the Mn and Ho moments for an applied field H.

applied field, the more stable 180° domain is the one shown in Fig. 8(a) in which the Ho1 with larger moments are parallel to the field. In both the AF1 and F2 phases, the intensity data determine the relative directions of the Ho and Mn moments even though they are orthogonal. In the F2 phase, when all the Ho are aligned along positive c, the moments of Mn atoms in alternate layers reverse with respect to their orientation in the AF1 phase. The configuration around the O3 atom at $z \approx 0$ is then as shown in Fig. 8(b), so that all the Mn and Ho1 moments point toward their nearest O3 neighbor. One may note that for the racemic twin magnetized in the same direction, the Ho1 moments would be reversed with respect to the coordination polyhedra, giving rise to a configuration with potentially different energy.

A surprising result, which indicates that the physical state of the system may be more complex than this simple model suggests, is the behavior of the polarization parameters. The values obtained are ≈0.25 for both phases and are nearly independent of either temperature or field. However, at the highest fields, when the fraction of the AF1 phase becomes very small, its polarization fraction tends to 1, indicating that the small residual fraction of the AF1 phase is a single 180° domain. The polarization constant for the F2 phase remains around 0.25. Naively, one would expect the polarization of the F2 phase to increase with increasing field as it is directly related to the net magnetization. It is possible that there is a depolarization effect associated with the boundaries between different phase and twin domains, which leads to the small polarization values.

V. CONCLUSIONS

The integrated intensity and polarized neutron asymmetry measurements show that the magnetic structure of $HoMnO_3$ changes, apparently nearly continuously, with increasing field from the zero field AF1 phase ($P6_3'cm'$) to a ferromagnetic F2 phase ($P6_3c'm'$) in which the triangular configuration of Mn moments in the (001) plane is maintained. There is also a significant variation with field in the ordered moments of Ho2 and Mn in the AF1 and F2 phases, respectively. The present results do not indicate any obvious origin for the wealth of anomalies observed in the dielectric

TABLE II. Comparison of the polarized neutron asymmetries observed at 2 K with those calculated from the model described in the text at 1, 2, and 4 T. F_{af} is the fraction of the AF1 phase and P_a and P_f the polarization parameters for the AF1 and F2 phases respectively.

	H=1 T, T=2 K		H=2 T, T=2 K		H=4 T, T=2 K	
$h\ k\ l$	A_{obs}	A_{calc}	A_{obs}	A_{calc}	A_{obs}	A_{calc}
1 0 0	−0.001(1)	0.000	−0.003(1)	−0.003		
2 0 0	−0.005(2)	0.000	−0.007(2)	−0.006		
3 0 0	0.051(2)	0.038	0.082(4)	0.088	0.149(6)	0.139
4 0 0	0.11(8)	0.000				
1 1 0	0.092(2)	0.114	0.188(3)	0.263	0.405(2)	0.434
2 1 0	0.05(2)	−0.005			0.015(5)	0.017
3 1 0	0.00(8)	−0.000				
4 1 0	0.058(2)	0.062	0.112(2)	0.133	0.232(3)	0.210
2 2 0	0.071(2)	0.086	0.148(8)	0.189	0.297(3)	0.303
1 0 1			−0.007(1)	0.000	0.002(3)	0.000
2 0 1			−0.002(4)	0.000	0.003(3)	0.000
1 1 1	0.280(6)	0.226	0.283(3)	0.277	0.317(4)	0.270
2 1 1	0.005(2)	0.034	0.016(2)	0.042	0.151(5)	0.156
3 1 1	0.004(5)	0.015	0.011(5)	0.011	0.032(7)	0.018
3 2 1	0.002(7)	−0.088	0.007(1)	−0.083	0.03(3)	−0.035
1 0 2	−0.002(2)	−0.016	0.001(5)	0.035	−0.440(9)	−0.357
2 0 2	0.064(2)	0.069	0.136(2)	0.131	0.408(4)	0.333
3 0 2	0.056(1)	0.082	0.129(3)	0.180	0.283(6)	0.289
4 0 2	−0.09(4)	−0.045				
1 1 2	−0.385(4)	−0.131	−0.323(2)	−0.159	−0.177(2)	−0.168
2 1 2	0.089(3)	0.078	0.163(6)	0.179	0.238(3)	0.191
4 1 2			−0.278(1)	−0.229	−0.184(4)	−0.236
2 2 2	−0.366(1)	−0.170	−0.314(7)	−0.215	−0.186(3)	−0.220
3 2 2	0.037(4)	0.034	0.063(3)	0.064	0.152(3)	0.116
F_{af}	0.26(6)		0.53(4)		0.937(9)	
P_a	0.20(6)		0.28(4)		1.000	
P_f	0.23(3)		0.28(2)		0.240(6)	

properties.[13] However, these dielectric properties probably depend more on the fine details of the atomic positions rather than on the magnetic structure. In particular, they will be closely related to the electronic polarization of the atoms and, consequently, to the Ho and O z parameters, which cannot be determined accurately in an experiment limited to $l \leqslant 2$. The signs of the polarized neutron asymmetries suggest that the Ho1 moment is enhanced when it points toward its unique close O3 neighbor, and the structures determined for both phases confirm a coupling between the orthogonal Mn and Ho moments, which ensures that the Mn and Ho1 moments all point either toward or away from their nearest O3 neighbor.

We have shown that combining the measurement of the polarization dependence of the neutron cross section with integrated intensities measured using unpolarized neutrons allows a more complete determination of a complex magnetic structure than could be obtained using either technique alone. In the present case, the magnitudes of the magnetic moments are obtained most precisely from the integrated intensity measurements, but only the phase sensitivity of the polarized neutron technique allows the particular configurations stabilized by a magnetic field to be identified.

APPENDIX A: MAGNETIC STRUCTURE FACTORS FOR $HoMnO_3$

$HoMnO_3$ has the space group $P6_3cm$ with the Mn atoms in 6(c) $(x,0,0)$ positions with $x \approx 1/3$ and the Ho1 and Ho2 atoms in $2a$ $(0,0,z_1)$ $z_1=0.279$ and 4b $(1/3,2/3,z_2)$ $z_2=0.2355$ positions, respectively. If $\mathbf{S}_1$, $\mathbf{S}_2$, and $\mathbf{S}_3$ are the magnetic moment vectors on the Mn atoms at $(x,0,0)$, $(0,x,0)$, and $(-x,-x,0)$, respectively, then, assuming $x=1/3$, the contribution to the magnetic structure factor $\mathbf{M}_{hkl}$ from the Mn layer at $z=0$ for different combinations of h and k is

$$\mathbf{S}_1 + \mathbf{S}_2 + \mathbf{S}_3, \quad h = 3n,\ k = 3n,$$

$$\frac{1}{2}(\mathbf{S}_1+\mathbf{S}_2+\mathbf{S}_3)(1+\imath\sqrt{3}),\quad h=3n+1,\ k=3n+1,$$

$$\frac{1}{2}(\mathbf{S}_1+\mathbf{S}_2+\mathbf{S}_3)(1-\imath\sqrt{3}),\quad h=3n+2,\ k=3n+2,$$

$$\mathbf{S}_3-\frac{1}{2}(\mathbf{S}_1+\mathbf{S}_2)+\frac{\imath\sqrt{3}}{2}(\mathbf{S}_1-\mathbf{S}_2),\quad h=3n+1,\ k=3n+2,$$

$$\mathbf{S}_2-\frac{1}{2}(\mathbf{S}_3+\mathbf{S}_1)+\frac{\imath\sqrt{3}}{2}(\mathbf{S}_3-\mathbf{S}_1),\quad h=3n+2,\ k=3n,$$

$$\mathbf{S}_1-\frac{1}{2}(\mathbf{S}_2+\mathbf{S}_3)+\frac{\imath\sqrt{3}}{2}(\mathbf{S}_2-\mathbf{S}_3),\quad h=3n,\ k=3n+1.$$

Since $\mathbf{S}_1+\mathbf{S}_2+\mathbf{S}_3=0$ for any arrangement of Mn moments in the 001 plane with a trigonal symmetry, only reflections for which h and k are mixed amongst $3n$, $3n+1$, and $3n+2$ have a Mn contribution. If the Mn moments at $x,y,0$ and $-x$, $-y,\frac{1}{2}$ are parallel the total Mn contribution to the magnetic structure factor for reflections $h=3n+1$, $k=3n+2$ is

$$2\mathbf{S}_3-\mathbf{S}_1-\mathbf{S}_2=3\mu_{\mathrm{Mn}}\|\mathbf{S}_3\quad\text{for } l \text{ even},$$

$$\sqrt{3}\imath(\mathbf{S}_1-\mathbf{S}_2)=3\mu_{\mathrm{Mn}}\perp\mathbf{S}_3\quad\text{for } l \text{ odd}.$$

The reverse is true if they are antiparallel.

Similarly, if $\mathbf{H}_1$ and $\mathbf{H}_2$ are the magnetic moment vectors on the Ho1 and Ho2 atoms with z close to $1/4$, their contribution to $\mathbf{M}_{hkl}$ for different values of $h+2k$ is

$$h+2k=3n,$$

$$2\mathbf{H}_1(-0.118+0.993\imath)+4\mathbf{H}_2(0.131+0.991\imath),\quad l=1,$$

$$2\mathbf{H}_1(-0.972-0.235\imath)+4\mathbf{H}_2(-0.965+0.261\imath),\quad l=2,$$

$$3n+1 \text{ or } 3n+2,$$

$$2\mathbf{H}_1(-0.118+0.993\imath)-2\mathbf{H}_2(0.131+0.991\imath),\quad l=1,$$

$$2\mathbf{H}_1(-0.972-0.235\imath)-2\mathbf{H}_2(-0.965+0.261\imath),\quad l=2.$$

The Ho atoms occur in pairs separated by $c/2$; hence, in the structure factor for the whole cell, the sum of each pair of moments contributes to l even and the difference to l odd reflections.

APPENDIX B: SYMMETRICAL EQUIVALENCE OF ASYMMETRY FACTORS

Consider a symmetry element $\mathcal{S}$ which relates the scattering density $\rho(\mathbf{r})$ at $\mathbf{r}$ to that at $\mathsf{R}\mathbf{r}+\mathbf{t}$, where R is a symmetry rotation and $\mathbf{t}$ a translation. The structure factor $F(\mathbf{k})$ is related to $F(\mathbf{k}')$, $\mathbf{k}'=\mathsf{R}^{-1}\mathbf{k}$ by

$$F(\mathbf{k}')=\int\rho(\mathbf{r})\exp(\imath\mathbf{k}'\cdot\mathbf{r})dr^3=\int\rho(\mathbf{r})\exp(\imath\mathbf{k}\cdot\mathsf{R}\mathbf{r})dr^3$$

$$=\int\rho(\mathsf{R}\mathbf{r}+\mathbf{t})\exp[\imath\mathbf{k}\cdot(\mathsf{R}\mathbf{r}+\mathbf{t})]dr^3.$$

If the symmetry $\mathcal{S}$ is maintained, then

$$\rho(\mathbf{r})=\rho(\mathsf{R}\mathbf{r}+\mathbf{t})\text{ and }F(\mathbf{k}')=F(\mathbf{k})\exp(\imath\mathbf{k}\cdot\mathbf{t}).$$

If it is lost, the structure factors can be expressed in terms of the mean and difference densities $\rho_S=[\rho(\mathbf{r})+\rho(\mathsf{R}\mathbf{r}+\mathbf{t})]/2$ and $\rho_D=[\rho(\mathbf{r})-\rho(\mathsf{R}\mathbf{r}+\mathbf{t})]/2$.

$$F(\mathbf{k})=\int[\rho_S(\mathbf{r})+\rho_D(\mathbf{r})]\exp(\imath\mathbf{k}\cdot\mathbf{r})dr^3=F_S(\mathbf{k})+F_D(\mathbf{k}),$$

$$F(\mathbf{k}')=\int[\rho_S(\mathbf{r})-\rho_D(\mathbf{r})]\exp[\imath\mathbf{k}\cdot(\mathbf{r}+\mathbf{t})dr^3]$$

$$=[F_S(\mathbf{k})-F_D(\mathbf{k})]\exp(\imath\mathbf{k}\cdot\mathbf{t}).$$

The polarized neutron asymmetry is given by $A=4\Re[N^*(\mathbf{k})M_z(\mathbf{k})]$, where $N(\mathbf{k})$ is the nuclear structure factor and $M_z(\mathbf{k})$ the component, parallel to the polarization direction, of the magnetic interaction vector. Using the same nomenclature, a symmetry element $\mathcal{S}$ in the magnetic structure implies

$$M_z(\mathbf{k})=M_{Sz}(\mathbf{k})=\pm M_z(\mathbf{k}')\exp(-\imath\mathbf{k}\cdot\mathbf{t}).$$

The sign depends on whether the z component of the interaction vector is $(-)$ or is not $(+)$ reversed by $\mathcal{S}$. If $\mathcal{S}$ is lost from the magnetic structure but retained in the nuclear one,

$$A(\mathbf{k})=2\Re[N^*(\mathbf{k})(M_{zS}(\mathbf{k})+M_{zD}(\mathbf{k}))],$$

$$A(\mathbf{k}')=\pm2\Re[N^*(\mathbf{k})(M_{zS}(\mathbf{k})-M_{zD}(\mathbf{k}))]\exp(\imath\mathbf{k}\cdot\mathbf{t}),$$

$$|A(\mathbf{k})|-|A(\mathbf{k}')|=4\Re[N^*(\mathbf{k})M_{zD}(\mathbf{k})].$$

Thus, any loss of symmetry in the magnetic structure implies a corresponding loss of symmetry in the asymmetries. Moreover, the contributions to the asymmetry due to the missing element $\mathcal{S}$ are equal and of opposite sign for the reflections $\mathbf{k}$ and $\mathbf{k}'$ related by $\mathcal{S}$ and, hence, will average to zero if the populations of the magnetic domains related by $\mathcal{S}$ are equal.

[1] T. H. O'Dell, *The Electrodynamics of Magneto-Electric Media* (North-Holland, Amsterdam, 1970).
[2] *Magnetoelectric Interaction Phenomenon in Crystals*, edited by A. J. Freeman and H. Schmid (Gordon and Breach, London, 1975).
[3] G. A. Smolenskii and I. E. Chupis, Sov. Phys. Usp. **25**, 475 (1982).
[4] T. Lottermoser, T. Lonkai, U. Amann, D. Hohlwein, J. Ihringer, and M. Fiebig, Nature (London) **430**, 541 (2004).
[5] T. Kimura, T. Goto, H. Shintani, K. Ishizaka, T. Arima, and Y. Tokura, Nature (London) **426**, 55 (2003).
[6] T. Kimura, G. Lawes, T. Goto, Y. Tokura, and A. P. Ramirez, Phys. Rev. B **71**, 224425 (2005).
[7] N. Hur, S. Park, P. A. Sharma, A. S. Ahn, S. Guha, and S.-W. Cheong, Nature (London) **429**, 392 (2004).
[8] P. Coeuré, F. Guinet, J. C. Peuzin, G. Bouisson, and E. F. Bertaut, in *Proceedings of the International Meeting on Ferroelectricity*, edited by V. Dvorak (Institute of Physics of the Czechoslovak Academy of Sciences, Prague, 1996), p. 332.
[9] M. Fiebig, D. Fröhlich, K. Kohn, St. Leute, Th. Lottermoser, V. V. Pavlov, and R. V. Pisarev, Phys. Rev. Lett. **84**, 5620 (2000).
[10] H. Sugie, N. Iwata, and K. Kohn, J. Phys. Soc. Jpn. **71**, 1558 (2002).
[11] O. P. Vajk, M. Kenzelmann, J. W. Lynn, S. B. Kim, and S.-W. Cheong, Phys. Rev. Lett.. **94**, 087601 (2005).
[12] B. Lorenz, A. P. Litvinchuk, M. M. Gospodinov, and C. W. Chu, Phys. Rev. Lett. **92**, 087204 (2004).
[13] F. Yen, C. R. dela Cruz, B. Lorenz, Y. Y. Sun, Y. Q. Wang, M. M. Gospodinov, and C. W. Chu, Phys. Rev. B **71**, 180407(R) (2005).
[14] J. Schweizer, in *Neutron Scattering from Magnetic Materials*, edited by T. Chatterji (Elsevier, Amsterdam, 2006), Chap. 4.
[15] P. J. Brown and T. Chatterji, J. Phys.: Condens. Matter **18**, 10085 (2006).